THE JOURNAL OF PHYSICAL CHEMISTRY Letters

Letter

pubs.acs.org/JPCL

Quantifying Lateral Inhomogeneity of Cholesterol-Containing Membranes

Celsa Díaz-Tejada, Igor Ariz-Extreme, Neha Awasthi, and Jochen S. Hub*

Georg-August-University Göttingen, Institute for Microbiology and Genetics, Justus-von-Liebig-Weg 11, 37077 Göttingen, Germany

Supporting Information

ABSTRACT: Lateral inhomogeneity plays a critical role for many properties of cholesterol-containing membranes, yet the thermodynamic forces involved in inhomogeneity remain poorly understood. Based on coarse-grained simulations of cholesterol in four increasingly unsaturated phospholipids, we computed lateral density fluctuations and free energies of domain formation, and we quantitatively relate those to variations in the chemical potential of cholesterol. Our simulations suggest that the lateral organization is dominated by weak repulsive cholesterol interactions, leading to a significantly more homogeneous distribution as compared to a two-dimensional ideal gas. Hence, phospholipids provide a "good" solvent for cholesterol. Unexpectedly, the degree of unsaturation of the phospholipid has only a minor effect on the lateral inhomogeneity of cholesterol in binary lipid mixtures. These results provide a link between functional properties and thermal fluctuations in lipid membranes.

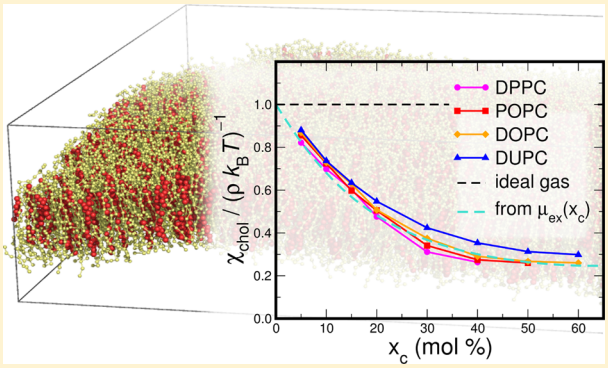

Cholesterol is a major component of the plasma membrane of animal cells, where it is present in concentrations up to 50 mol %. Cholesterol alters the structure of membranes by imposing a lower fraction of gauche rotamers in proximal phospholipid tails, thereby increasing the order and the packing density of the membrane.[1] Consequently, cholesterol modulates various physicochemical properties of membranes including bending moduli, lateral diffusion constants, or permeability.[2−6] In addition, the probability for the formation of water defects as required for ion permeation, and the activity of antimicrobial peptides are modulated by cholesterol.[7,8] The ordering effect of cholesterol molecules is spatially highly localized to proximal lipids.[9] Hence, in order to predict macroscopic properties of the membrane from the chemical interactions of cholesterol, a quantitative understanding of the lateral distribution of cholesterol is mandatory.

The lateral organization of cholesterol-containing membranes has been studied exhaustively with a focus on domain formation and phase separation in ternary lipid mixtures of cholesterol with saturated and unsaturated lipids.[10−13] From those studies it is well established that domain formation is driven by a more favorable enthalpy of cholesterol in saturated as compared to unsaturated membranes, typically by a few kilojoule per mole.[14−18] The lateral organization of binary lipid mixtures, which are the focus of the present study, has remained controversial. For mixtures of saturated lipids with cholesterol, a coexistence of liquid disordered/liquid ordered phases ($l_d + l_o$) was suggested for a certain composition and temperature range, but these mixtures exhibit, at best, nanoscopic domains.[19,20] In unsaturated lipids, no consensus was obtained whether a l_d/l_o coexistence provides an appropriate model.[21] However, even in the absence of well-defined domains, it is unclear whether cholesterol is homogeneously distributed in the membranes. Instead, merely by lateral diffusion, the local cholesterol concentration fluctuates, which might modulate the probability of rare cholesterol-dependent events such as pore formation or solute permeation.

A quantitative understanding for such density fluctuations in cholesterol-containing membranes has remained elusive. In particular, it is unclear whether the preferred interaction of cholesterol with saturated lipids also translates into different degrees of lateral inhomogeneity. To clarify these questions, here we used statistical theory of solutions to relate density fluctuations and domain formation to the chemical potential of cholesterol in different lipid mixtures. To investigate the effect of the phospholipid's unsaturation on lateral organization, we conducted coarse-grained (CG) molecular dynamics (MD) simulations of cholesterol in four phosphatidylcholine (PC) lipids of increasing unsaturation, namely, dipalmitoyl-PC (DPPC), palmitoyl-oleoyl-PC (POPC), dioleoyl-PC (DOPC), and di(cis−cis-9,12-octadecadienoyl)-PC (DUPC) (Figure 1). Molecular interactions were described by the Martini force field that models three to four heavy atoms as one CG bead.[22] The Martini model maintains some chemical specificity such as unsaturated hydrocarbon chains. Importantly, the model accounts for the preferred packing of cholesterol with saturated

Received: October 28, 2015
Accepted: November 17, 2015

DOI: 10.1021/acs.jpclett.5b02414
J. Phys. Chem. Lett. 2015, 6, 4799−4803

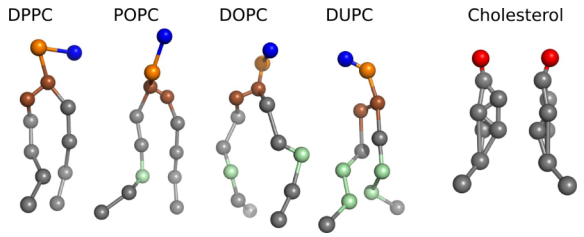

Figure 1. Coarse-grained representations of lipids considered in this study. Blue/orange: phospholipid head groups; brown: glycerol; gray: hydrocarbon; green: unsaturated groups; red: hydroxyl.

as compared to unsaturated chains, which allowed for successful simulations of phase separation in ternary mixtures.[23,24]

In order to quantify the thermodynamic forces involved in the lateral organization, we first computed potentials of mean force (PMFs) for moving one cholesterol molecule from a cholesterol-depleted into a cholesterol-enriched membrane domain. To this end, cholesterol-enriched slabs were enforced by imposing a flat-bottomed potential on the cholesterol molecules, whereas no restraints were applied to the phospholipids (Figure 2A/B). Technical details are provided in the Supporting Information (SI). PMFs were computed by umbrella sampling at 323 K and a constant pressure of 1 bar. The PMFs are shown in Figure 2C, where $y = 0$ corresponds to the center of the cholesterol slab, while $y \approx \pm 6$ nm corresponds to positions in the pure phospholipid region. The excess chemical potential difference $\Delta\mu_{ex}$ between the inside and outside of the cholesterol-enriched slab is plotted in Figure 2D, as taken from the PMFs. In all phospholipids, $\Delta\mu_{ex}$ was found to be positive, and it increases with the cholesterol mole fraction x_c. Hence, cholesterol is repelled from cholesterol-enriched domains, rationalizing why cholesterol does not spontaneously form domains in such binary mixtures.[25] Remarkably, the degree of saturation of the phospholipid showed little influence on $\Delta\mu_{ex}$ up to a cholesterol concentration of ~40 mol %, despite the more favorable packing of cholesterol with saturated tails. To further rationalize these findings, we computed the excess chemical potential μ_{ex} (or free energy of insertion) of cholesterol into 36 different lipid compositions using thermodynamic integration (Figure 2E; see SI for details). In agreement to experimental findings,[18,26] the simulations predict an increasing μ_{ex} with increasing number of double bonds in the lipid tails. Experimentally, the partition free energy of cholesterol into different PC membranes was found to vary by 1 to 3 kJ/mol, depending on the degree of unsaturations.[26−28] Thus, the difference of ~1.5 kJ/mol between DOPC and DPPC at zero cholesterol content are in reasonable agreement to experimental numbers (2E, orange vs magenta curves, $x_c = 0$). Contrary, μ_{ex} for DUPC seems to be larger than related experimental estimates for polyunsaturated lipids.[27,28] Thus, the DUPC model adopted in this study may be considered as a hypothetical lipid that exhibits particularly poor packing with cholesterol. However, Figure 2E confirms that the increase of μ_{ex} upon the addition of cholesterol, $(\partial\mu_{ex}/\partial x_c)_{P,T}$, is similar in different types of phospholipids, in agreement to the findings from the PMFs (Figure 2C/D). As shown in the following, the invariance of the *increase* of μ_{ex} with x_c translates into similar degrees of cholesterol inhomogeneity in different phospholipids.

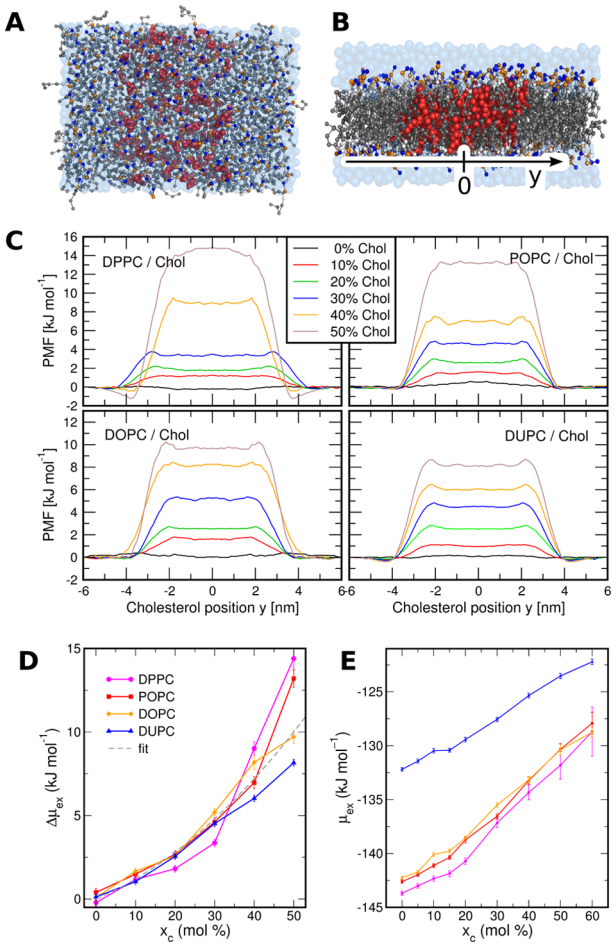

Figure 2. (A) Typical simulation system used to compute PMFs for lateral partitioning of cholesterol in top view and (B) side view. Red: cholesterol, restrained by a flat-bottomed potential in the central slab; gray/orange/black beads: phospholipids; transparent blue: water. (C) PMFs for moving a single cholesterol laterally across cholesterol-enriched slabs, embedded in different phospholipids, as indicated in the graphs. Color coding: cholesterol concentration (mol %) within the cholesterol-enriched slab. The *y*-axis is visualized as an arrow in panel B. (D) Excess chemical potential difference $\Delta\mu_{ex}$ for moving one cholesterol from the pure-phospholipid environment into the cholesterol-enriched slab, taken from the PMFs and hence computed by umbrella sampling. (E) Excess chemical potential (or free energy of insertion) of cholesterol in membranes of increasing cholesterol content, computed by thermodynamic integration. Color coding as in panel D.

We quantified the lateral inhomogeneity first from density fluctuations of cholesterol during equilibrium simulations. Fluctuation theory shows that, in the grand canonical ensemble, the isothermal compressibility of a liquid is related to density fluctuations via $\chi_T = \frac{\langle N_v^2\rangle - \langle N_v\rangle^2}{\langle N_v\rangle^2}\frac{V}{k_B T}$, where N_v is the particle number in the probe volume V, T denotes the temperature, k_B the Boltzmann constant, and $\langle\cdot\rangle$ is the ensemble average.[29] Analogously, we here consider the lateral two-dimensional (2D) compressibility of cholesterol $\chi_{chol} = \frac{\langle N_a^2\rangle - \langle N_a\rangle^2}{\langle N_a\rangle^2}\frac{A}{k_B T}$, where N_a denotes the cholesterol number in the probe area A. For noninteracting cholesterol molecules corresponding to a 2D ideal gas, $\chi_{chol} = (\rho k_B T)^{-1}$ would be expected, where ρ is the lateral cholesterol density. For interacting cholesterol mole-

DOI: 10.1021/acs.jpclett.5b02414
J. Phys. Chem. Lett. 2015, 6, 4799−4803

cules, statistical theory of solutions allows one to relate χ_{chol} to the chemical potential $\mu(x_c)$. Hence, we can relate fluctuations in equilibrium simulations to the single-cholesterol PMFs of Figure 2C. Assuming equilibrium between a probe area and the remaining simulation system, the mean-square fluctuation of the number of cholesterol molecules is given by[29]

$$\langle(\Delta N_a)^2\rangle = RT\left(\frac{\partial\mu(x_c)}{\partial N_a}\right)^{-1}_{P,T} \quad (1)$$

where R is the gas constant. Based on Figure 2D, we take for the chemical potential of cholesterol $\mu(x_c) = \mu^0 + RT \ln \rho + \Delta\mu_{ex}$. Here, we approximate $\Delta\mu_{ex} = m_1 x_c + m_2 x_c^2$, where $m_1 = 10$ kJ mol^{-1} and $m_2 = 20$ kJ mol^{-1} were chosen to match the $\Delta\mu_{ex}(x_c)$ curves (Figure 2D, dashed line). The cholesterol concentration is given by $x_c = N_a/(N_a + n_L)$, where n_L denotes the number of phospholipids inside the probe area. Evaluating eq 1 yields $\chi_{chol}/(\rho k_B T)^{-1} = \left[1 + \frac{x_c(1-x_c)}{RT}(m_1 + 2m_2 x_c)\right]^{-1}$, which contains the 2D ideal gas case for $m_1 = m_2 = 0$. The function is plotted in Figure 3B (dashed cyan curve). Hence,

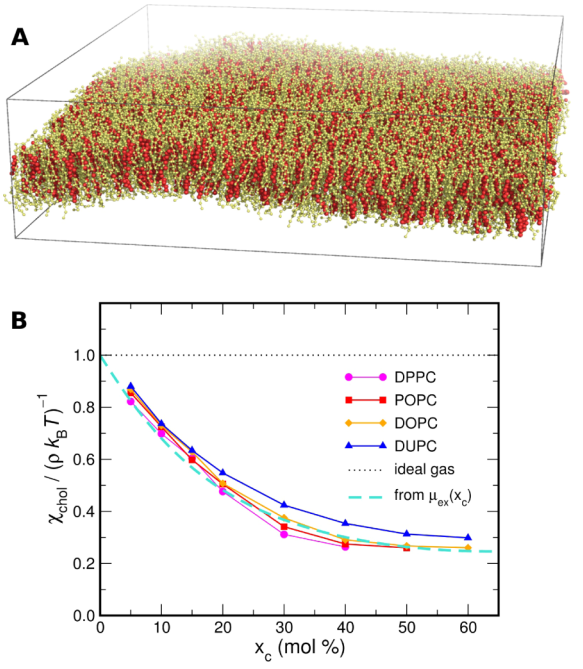

Figure 3. (A) Typical coarse-grained simulation system of 40 mol % cholesterol (red) in POPC (yellow), containing ~6000 lipid-cholesterol molecules and ~75.000 water beads (not shown for clarity). (B) Lateral compressibility χ_{chol}, normalized by the lateral cholesterol density ρ and $k_B T$. Colored lines: from MD simulations. Dashed cyan line: predicted from alterations of cholesterol chemical potential (Figure 2D). Dotted line: two-dimensional ideal gas.

the computed chemical potentials imply that $\chi_{chol}/(\rho k_B T)^{-1} < 1$ at all cholesterol concentrations in all phospholipids, suggesting that the cholesterol distribution is characterized by a lower compressibility or reduced fluctuations as compared to a 2D ideal gas. In other words, the lateral distribution of cholesterol is more homogeneous than the 2D ideal gas.

To validate these theoretical considerations, we computed χ_{chol} from equilibrium simulations of cholesterol-containing membranes at concentrations between 5 and 60 mol %, and embedded in one of the four different phospholipids shown in Figure 1. A typical simulation system used to compute χ_{chol} is shown in Figure 3A. Since we simulated in the NVT ensemble and not at constant chemical potential, we computed lateral density fluctuations at various probe areas A, and extrapolated to $1/A \to 0$ at small A (see SI for details).[30,31] Figure 3B (colored curves) presents $\chi_{chol}/(\rho k_B T)^{-1}$ as computed from the simulations. Favorable agreement with the theoretical estimate (Figure 3B, cyan) is found for all phospholipids, demonstrating that density fluctuations are consistent with the excess chemical potentials (Figure 2). The compressibility highly depends on the cholesterol content. At low cholesterol content, the cholesterol molecules hardly interact, thereby letting $\chi_{chol}/(\rho k_B T)^{-1} \to 1$, close to the ideal gas case. In contrast, with higher cholesterol content, density fluctuations are increasingly suppressed by repulsive cholesterol interactions, leading to a compressibility of ~1/3 of the ideal gas case. Notably, because $\Delta\mu_{ex}$ is similar in different lipids (Figure 2D), the compressibility hardly depends on the type of phospholipid.

How do the chemical potential differences presented above influence the formation of cholesterol-depleted domains? To address this, we computed the PMF of forming a circular cholesterol-depleted domain (Figure 4A/B), using the

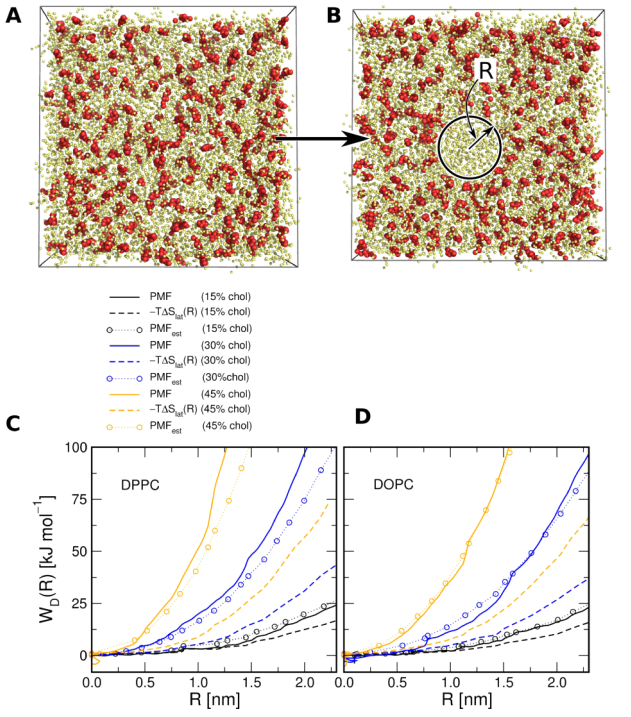

Figure 4. (A) Simulation system of DOPC (yellow) plus 30 mol % cholesterol (red). Water not shown for clarity. (B) Same system, but after creating a cholesterol-depleted domain of radius R at the center of the box (black circle). (C) PMFs $W_D(R)$ for creating a chlolesterol-depleted region in DPPC, and (D) in DOPC. Solid curves: PMFs from umbrella sampling; colors are indicated in the legend; dashed curves: loss of lateral entropy of cholesterol, $-T\Delta S_{lat}(R)$; circles: PMFs estimated as $W_\mu(R) - T\Delta S_{lat}(R)$.

collective radial reaction coordinate introduced by Tolpekina et al.[32] (SI for details). The PMFs as a function of domain radius R, $W_D(R)$, are presented in Figure 4C/D as solid curves. The PMFs rapidly increase with R, suggesting a low probability for spontaneous formation of cholesterol-depleted domains. As expected from the single-cholesterol PMFs of Figure 2C, the free energy of domain formation increases with cholesterol

DOI: 10.1021/acs.jpclett.5b02414
J. Phys. Chem. Lett. 2015, 6, 4799−4803

concentration. In addition, by comparing the PMFs from simulations in DPPC (Figure 4C) and DOPC (Figure 4D), we found again that the saturation of the phospholipid plays only a minor role, in line with the results presented above.

The PMFs for domain formation $W_D(R)$ can be related to $\Delta\mu_{ex}$ by decomposing the PMFs into two main components. First, the entropy of cholesterol in the lateral plane is reduced upon domain formation, which we quantified by the Shannon entropy $S_{lat}(R) = -k_B\int_{box} p_R(x,y) \ln p_R(x,y)\, dx\, dy$. Here, $p_R(x,y)$ is the lateral density of cholesterol at domain radius R. The entropic contribution $-T\Delta S_{lat}(R)$ computed from the simulation is shown as dashed curves Figure 4C/D. Notably, the loss of lateral entropy depends on the box area A_b, approximately via $\Delta S_{lat}(R) \approx k_B \ln(1 - \pi R^2/A_b)$. The second component originates from the fact that domain formation involves transfer of cholesterol molecules from a region of reduced cholesterol content into a region of higher cholesterol content. That component can be estimated from the excess chemical potential differences $\Delta\mu_{ex}$ (Figure 2D), which we take again as $\Delta\mu_{ex} = m_1 x_c + m_2 x_c^2$. Following the derivation in the SI, the second component to the PMFs is given by $\Delta W_\mu(R) = \pi R^2 \rho x_c\left(\frac{1}{2}m_1 + \frac{2}{3}m_2 x_c\right)$. The sum of the two components, $\Delta W_\mu(R) - T\Delta S_{lat}(R)$, is plotted as circles in Figure 4C/D.

The curves in Figure 4C/D demonstrate remarkable agreement between the PMFs $W_D(R)$ computed from the simulations (solid lines) and the estimate $\Delta W_\mu(R) - T\Delta S_{lat}(R)$ (circles), indicating that lateral organization of cholesterol was dominated by a combination of (i) lateral entropy and (ii) alterations in the chemical potential of cholesterol with cholesterol concentration. In addition, at low x_c, lateral entropy $S_{lat}(R)$ makes a major contribution to the free energy of domain formation (black curves in Figure 4C/D), suggesting that cholesterol behaves similar to a 2D ideal gas. At high x_c, in contrast, $S_{lat}(R)$ hardly contributes to the overall free energies, suggesting that the free energies of domain formation are dominated by repulsive cholesterol interactions (Figure 4C/D, blue and orange curves).

What are the structural mechanisms underlying the repulsive cholesterol interactions reported here? Previous studies established that cholesterol increases the packing density of the membrane by (i) reducing the area occupied per phospholipid (the condensing effect), and (ii) by filling the space below the phospholipid's glycerol groups with the bulky polycyclic groups.[1,33] Tighter packing increases the cost in free energy for adding another cholesterol molecule, leading to the repulsive interaction. In other words, considering cholesterol as solutes embedded in a solvent of phospholipid, we suggest that cholesterol molecules interact by modifying the structure of the solvent, leading to an indirect solvent-mediated repulsion. Because tighter packing is associated with lower enthalpy, we further suggest that the repulsive cholesterol interactions are of entropic origin.

To validate the results presented here, neutron scattering experiments of deuterated cholesterol will be required, similar to the work by Rheinstädter and co-workers,[20,34] but conducted at various x_c and in different phospholipids. Lateral structure factors derived from such experiments are related to radial distribution functions (Figure S2), which could be compared to the simulations shown here.

To conclude, we found that lateral entropy dominates the lateral organization only at very low cholesterol content. At higher cholesterol content, repulsive interactions between cholesterol become increasingly important. The lateral inhomogeneity can be quantified via chemical potentials, which we here translated into (i) free energies for the formation of cholesterol-depleted domains, and (ii) density fluctuations that are strongly suppressed as compared to the 2D ideal gas. Our analysis showed that the chemical potentials, the density fluctuations, and the free energies of domain formation were quantitatively consistent. The role of unsaturations were further analyzed by simulating cholesterol in four different increasingly unsaturated phospholipids. We found that the inhomogeneity is nearly independent of the degree of unsaturation, which might be unexpected noting that cholesterol preferentially partitions into membranes of saturated lipids.[3,17,35] However, we emphasized that partitioning is related to the magnitude of μ_{ex}, which clearly depends on lipid unsaturation,[26−28] whereas the lateral inhomogeneity is related to $\partial\mu_{ex}/\partial x_c$, which we here found to be nearly invariant with respect to unsaturation.

What are the functional implications of the present study? Local cholesterol concentrations modulate many membrane properties such as lipid packing, bending moduli, membrane curvature, line tension, or diffusion constants.[3−6] Localized events related to such properties, such as defect formation or solute permeation, are therefore expected to strongly depend on the variance of local cholesterol concentrations and, hence, on lateral inhomogeneity. To quantify such effects, free energies of defect formation or solute permeation could be related to the size of cholesterol-depleted domains. In addition, it will be highly interesting to investigate the inhomogeneity of more complex lipid mixtures or of membranes close to phase transition temperatures. Such future calculations, building upon the work presented here, provide a route to gain quantitative understanding of the functional role of lateral inhomogeneity in membrane biophysics.

■ ASSOCIATED CONTENT

Supporting Information

The Supporting Information is available free of charge on the ACS Publications website at DOI: 10.1021/acs.jpclett.5b02414.

Computational and methodological details, as well as three supporting figures (PDF)

■ AUTHOR INFORMATION

Corresponding Author

*Phone: +49-551-3914189 E-mail: jhub@gwdg.de.

Notes

The authors declare no competing financial interest.

■ ACKNOWLEDGMENTS

We are grateful to Marcus Müller and Kalina Atkovska for critically reading the manuscript, and we thank Marcus Müller for helpful discussions. This study was supported by the Deutsche Forschungsgemeinschaft (HU 1971/1-1 and SFB 803/A12). N.A. was supported by a Dorothea Schlözer fellowship.

■ REFERENCES

(1) Róg, T.; Pasenkiewicz-Gierula, M.; Vattulainen, I.; Karttunen, M. Ordering Effects of Cholesterol and Its Analogues. *Biochim. Biophys. Acta, Biomembr.* **2009**, *1788*, 97−121.

DOI: 10.1021/acs.jpclett.5b02414
J. Phys. Chem. Lett. 2015, 6, 4799−4803

(2) Finkelstein, A.; Cass, A. Effect of Cholesterol on the Water Permeability of Thin Lipid Membranes. *Nature* **1967**, *216*, 717−718.
(3) Pan, J.; Mills, T. T.; Tristram-Nagle, S.; Nagle, J. F. Cholesterol Perturbs Lipid Bilayers Nonuniversally. *Phys. Rev. Lett.* **2008**, *100*, 198103.
(4) Rubenstein, J.; Smith, B. A.; McConnell, H. M. Lateral Diffusion in Binary Mixtures of Cholesterol and Phosphatidylcholines. *Proc. Natl. Acad. Sci. U. S. A.* **1979**, *76*, 15−18.
(5) Miao, L.; Nielsen, M.; Thewalt, J.; Ipsen, J. H.; Bloom, M.; Zuckermann, M. J.; Mouritsen, O. G. From Lanosterol to Cholesterol: Structural Evolution and Differential Effects on Lipid Bilayers. *Biophys. J.* **2002**, *82*, 1429−1444.
(6) Karatekin, E.; Sandre, O.; Guitouni, H.; Borghi, N.; Puech, P.-H.; Brochard-Wyart, F. Cascades of Transient Pores in Giant Vesicles: Line Tension and Transport. *Biophys. J.* **2003**, *84*, 1734−1749.
(7) Lande, M. B.; Donovan, J. M.; Zeidel, M. L. The Relationship Between Membrane Fluidity and Permeabilities to Water, Solutes, Ammonia, and Protons. *J. Gen. Physiol.* **1995**, *106*, 67−84.
(8) Zasloff, M. Antimicrobial Peptides of Multicellular Organisms. *Nature* **2002**, *415*, 389−395.
(9) Jedlovszky, P.; Medvedev, N. N.; Mezei, M. Effect of Cholesterol on the Properties of Phospholipid Membranes. 3. Local Lateral Structure. *J. Phys. Chem. B* **2004**, *108*, 465−472.
(10) Marsh, D. Cholesterol-Induced Fluid Membrane Domains: A Compendium of Lipid-Raft Ternary Phase Diagrams. *Biochim. Biophys. Acta, Biomembr.* **2009**, *1788*, 2114−2123.
(11) Pandit, S. A.; Scott, H. L. Multiscale Simulations of Heterogeneous Model Membranes. *Biochim. Biophys. Acta, Biomembr.* **2009**, *1788*, 136−148.
(12) Berkowitz, M. L. Detailed Molecular Dynamics Simulations of Model Biological Membranes Containing Cholesterol. *Biochim. Biophys. Acta, Biomembr.* **2009**, *1788*, 86−96.
(13) Komura, S.; Andelman, D. Physical Aspects of Heterogeneities in Multi-Component Lipid Membranes. *Adv. Colloid Interface Sci.* **2014**, *208*, 34−46.
(14) Ali, M. R.; Cheng, K. H.; Huang, J. Assess the Nature of Cholesterol-Lipid Interactions Through the Chemical Potential of Cholesterol in Phosphatidylcholine Bilayers. Proc. *Proc. Natl. Acad. Sci. U. S. A.* **2007**, *104*, 5372−5377.
(15) Veatch, S. L.; Keller, S. L. Organization in Lipid Membranes Containing Cholesterol. *Phys. Rev. Lett.* **2002**, *89*, 268101.
(16) Tsamaloukas, A.; Szadkowska, H.; Heerklotz, H. Thermodynamic Comparison of the Interactions of Cholesterol with Unsaturated Phospholipid and Sphingomyelins. *Biophys. J.* **2006**, *90*, 4479−4487.
(17) Pandit, S. A.; Chiu, S.-W.; Jakobsson, E.; Grama, A.; Scott, H. L. Cholesterol Packing Around Lipids with Saturated and Unsaturated Chains: A Simulation Study. *Langmuir* **2008**, *24*, 6858−6865.
(18) Almeida, P. F. Thermodynamics of Lipid Interactions in Complex Bilayers. *Biochim. Biophys. Acta, Biomembr.* **2009**, *1788*, 72−85.
(19) Marsh, D. Liquid-Ordered Phases Induced by Cholesterol: A Compendium of Binary Phase Diagrams. *Biochim. Biophys. Acta, Biomembr.* **2010**, *1798*, 688−699.
(20) Toppozini, L.; Meinhardt, S.; Armstrong, C. L.; Yamani, Z.; Kučerka, N.; Schmid, F.; Rheinstädter, M. C. Structure of Cholesterol in Lipid Rafts. *Phys. Rev. Lett.* **2014**, *113*, 228101.
(21) Heerklotz, H.; Tsamaloukas, A. Gradual Change or Phase Transition: Characterizing Fluid Lipid-Cholesterol Membranes on the Basis of Thermal Volume Changes. *Biophys. J.* **2006**, *91*, 600−607.
(22) Marrink, S. J.; Risselada, H. J.; Yefimov, S.; Tieleman, D. P.; de Vries, A. H. The MARTINI Force Field: Coarse Grained Model for Biomolecular Simulations. *J. Phys. Chem. B* **2007**, *111*, 7812−7824.
(23) Risselada, H. J.; Marrink, S. J. The Molecular Face of Lipid Rafts in Model Membranes. *Proc. Natl. Acad. Sci. U. S. A.* **2008**, *105*, 17367−17372.
(24) Schäfer, L. V.; de Jong, D. H.; Holt, A.; Rzepiela, A. J.; de Vries, A. H.; Poolman, B.; Killian, J. A.; Marrink, S. J. Lipid Packing Drives the Segregation of Transmembrane Helices into Disordered Lipid Domains in Model Membranes. *Proc. Natl. Acad. Sci. U. S. A.* **2011**, *108*, 1343−1348.
(25) Waheed, Q.; Tjörnhammar, R.; Edholm, O. Phase Transitions in Coarse-Grained Lipid Bilayers Containing Cholesterol by Molecular Dynamics Simulations. *Biophys. J.* **2012**, *103*, 2125−2133.
(26) Halling, K. K.; Ramstedt, B.; Nyström, J. H.; Slotte, J. P.; Nyholm, T. K. Cholesterol Interactions with Fluid-Phase Phospholipids: Effect on the Lateral Organization of the Bilayer. *Biophys. J.* **2008**, *95*, 3861−3871.
(27) Leventis, R.; Silvius, J. R. Use of Cyclodextrins to Monitor Transbilayer Movement and Differential Lipid Affinities of Cholesterol. *Biophys. J.* **2001**, *81*, 2257−2267.
(28) Niu, S.-L.; Litman, B. J. Determination of Membrane Cholesterol Partition Coefficient Using a Lipid Vesicle-Cyclodextrin Binary System: Effect of Phospholipid Acyl Chain Unsaturation and Headgroup Composition. *Biophys. J.* **2002**, *83*, 3408−3415.
(29) Landau, L.; Lifshitz, E. M. *Statistical Physics*; Pergamon Press: London, 1958.
(30) Rovere, M.; Hermann, D.; Binder, K. Block Density Distribution Function Analysis of Two-Dimensional Lennard-Jones Fluids. *Europhys. Lett.* **1988**, *6*, 585.
(31) Müller, M.; Schick, M. Structure and Nucleation of Pores in Polymeric Bilayers: A Monte Carlo Simulation. *J. Chem. Phys.* **1996**, *105*, 8282−8292.
(32) Tolpekina, T.; Den Otter, W.; Briels, W. Nucleation Free Energy of Pore Formation in an Amphiphilic Bilayer Studied by Molecular Dynamics Simulations. *J. Chem. Phys.* **2004**, *121*, 12060−12066.
(33) Wennberg, C.; van der Spoel, D.; Hub, J. S. Large Influence of Cholesterol on Solute Partitioning into Lipid Membranes. *J. Am. Chem. Soc.* **2012**, *134*, 5351−5361.
(34) Meinhardt, S.; Vink, R. L.; Schmid, F. Monolayer Curvature Stabilizes Nanoscale Raft Domains in Mixed Lipid Bilayers. *Proc. Natl. Acad. Sci. U. S. A.* **2013**, *110*, 4476−4481.
(35) Marrink, S. J.; de Vries, A. H.; Harroun, T. A.; Katsaras, J.; Wassall, S. R. Cholesterol Shows Preference for the Interior of Polyunsaturated Lipid Membranes. *J. Am. Chem. Soc.* **2008**, *130*, 10−11.

DOI: 10.1021/acs.jpclett.5b02414
J. Phys. Chem. Lett. 2015, 6, 4799−4803